Check for updates

ChemPhysChem

Research Article
doi.org/10.1002/cphc.202300407

Chemistry Europe
European Chemical Societies Publishing

www.chemphyschem.org

# Pair Distribution Function from Liquid Jet Nanoparticle Suspension using Femtosecond X-ray Pulses

Lise Joost Støckler,[a] Rasmus Stubkjær Christensen,[a] Magnus Kløve,[a] Andreas Dueholm Bertelsen,[a] Anders Bæk Borup,[a] Lennard Krause,[a] Seiya Takahashi,[b] Tomoki Fujita,[a, b] Hidetaka Kasai,[b] Ichiro Inoue,[c] Eiji Nishibori,[b] and Bo Brummerstedt Iversen*[a]

X-ray scattering data measured on femtosecond timescales at the SACLA X-ray Free Electron Laser (XFEL) facility on a suspension of $HfO_2$ nanoparticles in a liquid jet were used for pair distribution function (PDF) analysis. Despite a non-optimal experimental setup resulting in a modest $Q_{max}$ of ~8 $Å^{-1}$, a promising PDF was obtained. The main features were reproduced when comparing the XFEL PDF to a PDF obtained from data measured at the PETRA III synchrotron light source. Refining structural parameters such as unit cell dimension and particle size from the XFEL PDF provided reliable values. Although the reachable $Q_{max}$ limited the obtainable information, the present results indicate that good quality PDFs can be obtained on femtosecond timescales if the experimental conditions are further optimized. The study therefore encourages a new direction in ultrafast structural science where structural features of amorphous and disordered systems can be studied.

Nanocrystals constitute a cornerstone in modern technologies such as energy applications and catalysis.[1] Understanding nanocrystal nucleation, growth, and structure is vital for rationally designing and optimizing materials. For time and space averaged structural characterization of crystalline materials, analysis of Bragg intensities is arguably the most successful method. However, for poorly crystalline systems such as nanoparticles, using the Pair Distribution Function (PDF) has become an essential tool.[2] The PDF is obtained by Fourier transforming the coherently scattered radiation, *i.e.*, both the Bragg and the diffuse scattering.[2] The PDF can be interpreted as a scattering power weighted histogram of interatomic distances, and it provides a fingerprint of the atomic structure of any sample irrespective of its state. Time-resolved (*i.e., in situ)* PDF studies of chemical and physical processes allow for studies of structural dynamics in real time.[3]

In general, data with wide Q-ranges (2θ-ranges) are required to obtain reliable PDFs, and this necessitates use of intense, high-energy X-rays.[2] Synchrotron based *in situ* PDF studies have explored the syntheses of nanocrystals by elaborating the coordination chemistry of the solvated metal ion complexes as well as the atomic structures of the final nanoparticles.[4] Recently, the time resolutions of these studies have reached milliseconds at 4$^{th}$ generation synchrotron sources such as MAX IV.[5] However, this is still limiting the structural understanding to time and ensemble averaged structural motifs. Electronic excitations or chemical reactions such as ligand rearrangements occur on much faster timescales down to pico- or femtoseconds.[6] To follow the initial breaking and making of bonds with Å-resolution, the experimental timescale must match the ultrafast timescales of the underlying system.[7] Although some synchrotron facilities can deliver pulsed radiation on picosecond timescales, the number of photons delivered per pulse is inadequate to facilitate the creation of "molecular movies" with a high enough spatiotemporal resolution to follow such ultrafast processes.

Extremely brilliant X-ray pulses on timescales down to femtoseconds can be produced at X-ray Free Electron Laser (XFEL) facilities,[8] and X-ray crystallography on macromolecular compounds has already seen significant progress through XFEL studies.[9] XFEL PDF studies would provide access to unprecedented spatial details of ultrafast processes irrespective of the state of the systems, making it possible to reveal reaction pathways with atomistic detail and uncover initial steps of reaction mechanisms. Most XFELs deliver soft X-rays, explaining the lack of existing XFEL PDF studies. However, some XFELs can now deliver relatively hard X-rays, and at the SPring-8 Angstrom

[a] L. J. Støckler, R. S. Christensen, M. Kløve, A. D. Bertelsen, A. B. Borup, Prof. Dr. L. Krause, Dr. T. Fujita, Prof. Dr. Dr. Dr. B. B. Iversen
Center for Integrated Materials Research, Department of Chemistry and iNANO
Aarhus University
Langelandsgade 140, Aarhus, 8000 (Denmark)
E-mail: bo@chem.au.dk

[b] S. Takahashi, Dr. T. Fujita, Prof. Dr. H. Kasai, Prof. Dr. E. Nishibori
Department of Physics, Faculty of Pure and Applied Sciences and TREMS
University of Tsukuba
1-1-1, Tennodai, Tsukuba, Ibaraki, 305-8571 (Japan)

[c] Dr. I. Inoue
RIKEN SPring-8 Center
1-1-1, Kouto, Sayo-cho, Sayo-gun, Hyogo, 679-5148 (Japan)

Supporting information for this article is available on the WWW under https://doi.org/10.1002/cphc.202300407

© 2023 The Authors. ChemPhysChem published by Wiley-VCH GmbH. This is an open access article under the terms of the Creative Commons Attribution Non-Commercial NoDerivs License, which permits use and distribution in any medium, provided the original work is properly cited, the use is non-commercial and no modifications or adaptations are made.



© 2023 The Authors. ChemPhysChem published by Wiley-VCH GmbH

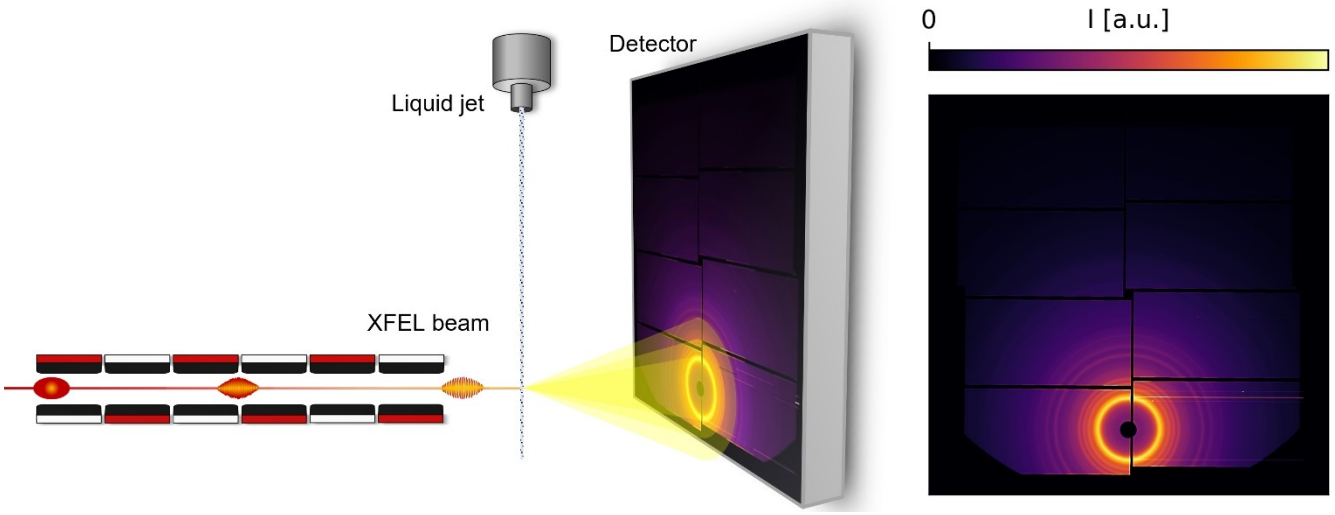


**Figure 1.** a) Sketch of the experimental setup using the liquid jet at SACLA. b) Data frame of a suspension of $HfO_2$ nanoparticles in EG from a single femtosecond X-ray pulse.

Compact free-electron LAser (SACLA) in Japan, X-ray energies of up to 22 keV can be achieved.[10] Here, a PDF study of data measured on femtosecond timescales at SACLA on a suspension of $HfO_2$ nanoparticles in a liquid jet setup is presented. Several critical issues were encountered during the data analysis due to non-optimal experimental conditions, a difficult calibration process, and challenging background measurements. Despite these problems, refinement of the obtained XFEL PDF provides reliable unit cell dimensions and crystallite sizes. The results clearly indicate that high quality femtosecond PDF data can potentially be obtained if relatively straightforward improvements to the experimental conditions are implemented. This study therefore establishes optimism regarding the future of ultrafast structural science on non-crystalline systems.

The XFEL data were measured at the BL2 beamline at SACLA in transmission geometry using a liquid jet setup as sketched in Figure 1a with an 8-module Multi-Port Charge-Coupled Device (MPCCD) Octal Phase-III detector.[11] The reliability of the information obtained from a PDF analysis benefits from a wide Q-range. At this beamtime, the setup was fixed, resulting in a modest $Q_{max}$ of ~8 $Å^{-1}$. A more detailed description of the experimental setup is provided in the 'Experimental Section' and in 'Supporting Information' (SI) sec. 1. The only working sample (discussed in more detail in SI sec. 1) consisted of $HfO_2$ nanoparticles suspended in ethylene glycol (EG) to a concentration of 0.2 M. A data frame from a single femtosecond X-ray pulse is shown in Figure 1b, and it exhibits clear powder rings and a good signal-to-noise ratio. In the interest of reducing statistical noise, 50 raw data frames were summed for the data analysis as is custom for serial crystallography. Each of these frames are measured with a less than 10 fs XFEL pulse.

To establish a model for fair evaluation of the XFEL PDF of $HfO_2$, the XFEL data were analyzed in reciprocal space and subsequently compared with Powder X-ray Diffraction (PXRD) data measured on the same batch of $HfO_2$ nanoparticles using an in-house diffractometer (experimental details are provided in the 'Experimental Section'; details about the refinement are given in SI sec. 3). According to the refinement of the laboratory data, the $HfO_2$ nanoparticles could be modelled using the monoclinic space group $P2_1/c$ with a = 5.20(3) Å, b = 5.18(2) Å, c = 5.28(2) Å, and β = 99.01(5)° (summarized in Table 1). The unit cell metrics and the space group agree with literature (Ruh *et al.* (ICSD: 27313), see Table 1 and SI sec. 2).[12]

The XFEL data were initially modelled in reciprocal space by Le Bail fitting in the 2θ-range 8–56.5° using TOPAS v. 7[13] (Figure 2). The background was modelled using a measurement of the liquid jet containing EG exclusively. The measured EG data had to be scaled to match the XFEL data of $HfO_2$. The elevated background in the XFEL data of $HfO_2$ was probably due to fluorescence as the X-ray energy of the beam (15 keV) was relatively close to the L-absorption edge of Hf (~11 keV).[14] The contribution from the fluorescence should be 2θ-independent and should not affect the Le Bail fit.

When reducing the 2D scattering images to 1D (*i.e.*, to obtain the PXRD pattern or the PDF), a measurement of a reference material collected using the same experimental setup is preferred to accurately calibrate the sample-to-detector distance, beam position, and detector rotations. Moreover, the measurement of the reference material is necessary to account

**Table 1.** Unit cell dimensions and spherical crystallite sizes of the $HfO_2$ nanoparticles from refinement of laboratory data, from refinement of femtosecond XFEL data, and from literature.

| | Literature[12] | Laboratory | XFEL PXRD | XFEL PDF |
|---|---|---|---|---|
| a [Å] | 5.1126 | 5.20(3) | 5.188(3) | 5.161(1) |
| b [Å] | 5.1722 | 5.18(2) | 5.167(2) | 5.204(2) |
| c [Å] | 5.2948 | 5.28(2) | 5.289(2) | 5.342(2) |
| β [Å] | 99.18 | 99.01(5) | 99.05(5) | 99.88(3) |
| V [$Å^3$] | 138.2 | 141(1) | 140(1) | 141.36(7) |
| Size [nm] | – | 4.08(2) | 4.13(3) | 4.38(3) |


© 2023 The Authors. ChemPhysChem published by Wiley-VCH GmbH

14397641, 2023, 23, Downloaded from https://chemistry-europe.onlinelibrary.wiley.com/doi/10.1002/cphc.202300407 by Cochrane Germany, Wiley Online Library on [15/12/2023]. See the Terms and Conditions (https://onlinelibrary.wiley.com/terms-and-conditions) on Wiley Online Library for rules of use; OA articles are governed by the applicable Creative Commons License

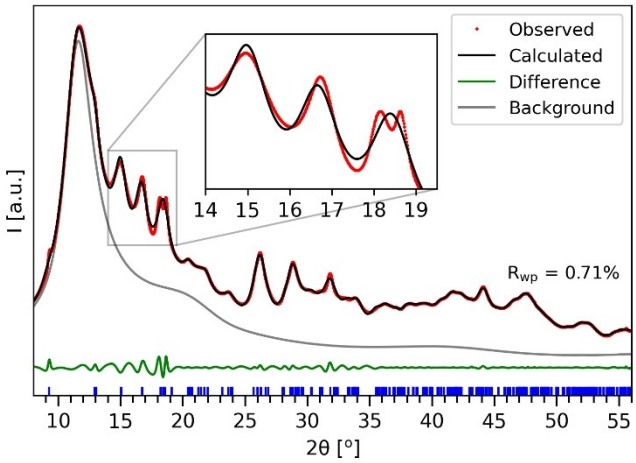


**Figure 2.** XFEL data of $HfO_2$ (red), Le Bail fit using a spherical model for the crystallite size (black), background (grey), and difference curve (green).

for the instrumental effects on the peak size broadening when analyzing nanoparticle sizes. However, the measured reference data could not be used for calibration, so the instrument resolution had to be determined from $LaB_6$ capillary data. These calibration conditions were not ideal, and the resulting complications encountered during calibration as well as real and reciprocal space refinements of the data of the reference material are discussed in more detail in SI sec. 4–6. Furthermore, careful masking had to be employed to account for irregularities in the intensity distributions observed on the detector frames of the XFEL data of $HfO_2$ (discussed in SI sec. 7–9).

The Le Bail fit of the XFEL data of $HfO_2$ accounts for all the expected reflections (Figure 2), however, the peak shapes clearly vary. This effect is not adequately described by the model (see for instance the two sharp peaks at 2θ~9° and 19°). The variation in peak shape was also encountered when modelling the laboratory data (see SI sec. 3). These observations could indicate anisotropic nanoparticle sizes, possibly caused by a preferred growth direction of the layered $HfO_2$ structure (see Figure S1). In fact, the two peaks at ~9° and 19° correspond to the (100) and (200) planes, respectively. Thus, different anisotropic crystallite models were tested, and an anisotropic cuboid model showed the best agreement (described in SI sec. 8). This anisotropic model resulted in an improved residual with $R_{wp}$ decreasing from 0.71 % to 0.51 % (Figure 2 and Figure S10). The anisotropic model gave unit cell dimensions of a = 5.140(5) Å, b = 5.189(7) Å, c = 5.282(4) Å, and β = 98.92(3)°, in reasonable agreement with literature[12] and very similar to the values obtained from refining the laboratory data (see Table 1). A cuboidal-shaped crystallites size of ~8.6 nm × 1.0 nm × 5.8 nm was obtained from the Le Bail refinement of the XFEL data (see SI sec. 8). Again, excellent agreement was obtained with the laboratory PXRD values of ~8.2 nm × 1.1 nm × 3.4 nm (see SI sec. 3). However, the anisotropic fits were not perfect (see Figure S10 and Figure S2b), and it should be kept in mind that 1 nm corresponds to approx. two unit cell lengths. Note also that the extracted sizes do not take contribution from strain into account.

For simplicity, an isotropic crystallite morphology model is assumed from hereon. A small change in unit cell dimensions is observed when using the isotropic crystallite model for the Le Bail refinement of the XFEL data compared with the anisotropic model. The obtained unit cell is tabulated in Table 1. The change in the unit cell parameters is most pronounced for the a-axis, further indicating anisotropy related to the (h00) reflections. A spherical crystallite size of ~4.1 nm was found from the Le Bail refinements of the XFEL data (see Table 1), which was the exact same size as obtained from refining the laboratory data. This value is in good agreement with previously published sizes of $HfO_2$ nanoparticles obtained from similar synthesis methods.[4c]

The XFEL data of $HfO_2$ calibrated with the $LaB_6$ capillary data were Fourier transformed in xPDFsuite[15] using a data range from $Q_{min} = 0.9$ Å$^{-1}$ to $Q_{max} = 7.9$ Å$^{-1}$. In xPDFsuite, the background correction was carried out using the measured EG background scaled accordingly prior to the Fourier transformation. Usually, background contributions from fluorescence can be handled by the $Q_{max,instrumental}$ and $r_{poly}$ parameters when calculating the PDF as these parameters correct for contributions from incoherently or inelastically scattered intensity. However, in the present case, the determination of a reliable correction was complicated by the limited Q-range. To obtain a reasonable scattering structure function, S(Q), $Q_{max,instrumental}$ and $r_{poly}$ were set equal to 8.2 Å$^{-1}$ and 1.5 Å, respectively. The value of $r_{poly}$ was guided by the shortest interatomic distance in the layered $HfO_2$ structure being ~2 Å. In $HfO_2$, $Hf^{4+}$ coordinates to seven oxygen ions at distances of either 2.09 Å or 2.21 Å, and the nearest Hf–Hf distances are 3.44 Å and 3.92 Å (see Figure S1).[12] The obtained PDF for the XFEL data of $HfO_2$ is shown in Figure 3.

Figure 3 also shows a PDF obtained from data measured at the P21.1 beamline at the PETRA III synchrotron light source (DESY, Hamburg, Germany) on a capillary containing $HfO_2$ nanoparticles in methanol. At PETRA III, data were collected on a 2D PerkinElmer XRD1621 detector at a sample-to-detector distance of ~30 cm with an X-ray energy of ~100 keV. In this case, the nanoparticles were formed *in situ* by heating a $HfCl_4$ precursor solution to 300°C under an applied pressure of ~3600 PSI. To ease the comparison with the Q-limited XFEL PDF, the same Q-range, $r_{poly}$, and $Q_{max,instrumental}$ parameters were selected for the synchrotron PDF. Moreover, the PDFs were normalized to the peak at ~3.4 Å.

The XFEL PDF clearly reproduces most of the features observed in the synchrotron PDF. However, the modest $Q_{max}$ of 7.9 Å$^{-1}$ makes the interatomic distances unreliable; the theoretical spatial resolution at this $\Delta r \sim \pi/Q_{max} \sim 0.40$ Å. Only the most intense peak at ~3.4 Å, which originates from the shortest Hf–Hf distance, is visible and correctly positioned in the XFEL PDF. The S(Q) function of the synchrotron data contained distinct features at higher Q-values than 8 Å$^{-1}$, and Figure 4 illustrates the PDF quality obtainable when using different $Q_{max}$-values for the synchrotron data while keeping all other parameters constant (here, $Q_{max,instrumental} = 30$ Å$^{-1}$). A comparison


© 2023 The Authors. ChemPhysChem published by Wiley-VCH GmbH

14397641, 2023, 23, Downloaded from https://chemistry-europe.onlinelibrary.wiley.com/doi/10.1002/cphc.202300407 by Cochrane Germany, Wiley Online Library on [15/12/2023]. See the Terms and Conditions (https://onlinelibrary.wiley.com/terms-and-conditions) on Wiley Online Library for rules of use; OA articles are governed by the applicable Creative Commons License

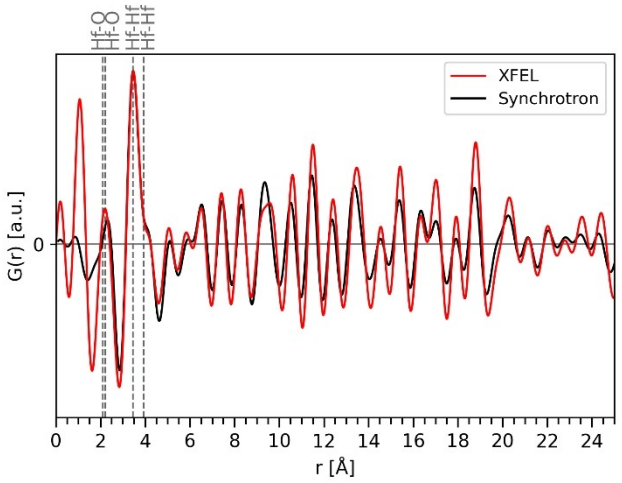


**Figure 3.** PDF obtained from data measured on a suspension of $HfO_2$ nanoparticles at an XFEL in a liquid jet (red) and at a synchrotron in a capillary (black). The two shortest Hf–O and Hf–Hf distances are indicated as reported by Ruh *et al.*[12] The two PDFs were normalized to the Hf–Hf distance at ~3.4 Å for fair comparison. Notice that the region below the shortest distance of ~2 Å is mostly noise which is not uncommon as errors often accumulate here.[2]

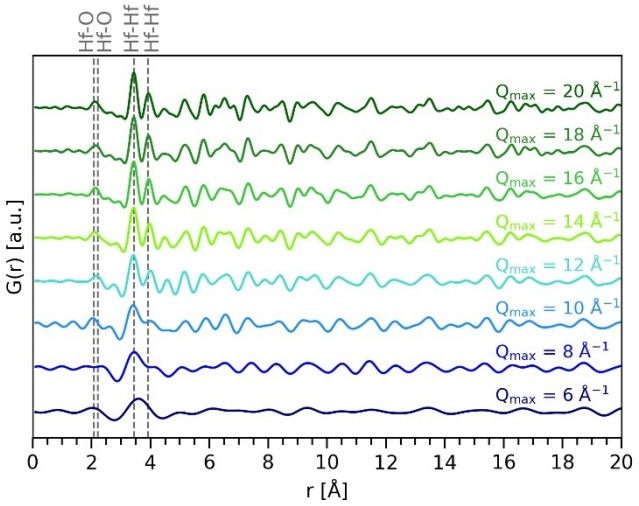


**Figure 4.** PDFs obtained from total scattering data measured at the PETRA III synchrotron facility on $HfO_2$ nanoparticles in methanol with different $Q_{max}$-values. The two shortest Hf–O and Hf–Hf distances are indicated.

of the PDFs obtained with a $Q_{max}$ of 8 $Å^{-1}$ and 20 $Å^{-1}$ clearly indicates that the information is limited in the XFEL data due to the limited $Q_{max}$. The two shortest Hf–Hf distances of the $HfO_2$ structure are well resolved at $Q_{max}$-values as low as 12–14 $Å^{-1}$ for the typical *in situ* synchrotron data ($\Delta r$ ~0.26–0.22 Å), but they smear out at $Q_{max}$-values below 10 $Å^{-1}$. The two Hf–O distances 0.12 Å apart cannot be resolved even at a $Q_{max}$ of 20 $Å^{-1}$ ($\Delta r$ ~0.16 Å). It is noteworthy that the noise level in the XFEL PDF is reasonably low at higher r-values. When measuring PDF data with millisecond resolution at MAX IV, the poorer counting statistics lead to noisy PDF features.[4] The instrument at SACLA is clearly capable of measuring total scattering data of sufficient signal to noise ratio to obtain reliable PDFs.

The higher noise level at lower r-values in the XFEL PDF compared to the synchrotron PDF is expected to be related to the fluorescence correction. As the data is treated over a very limited Q-range, it is very difficult to be certain of the correct background subtraction. Figure 5 shows the reduced structure functions, F(Q), from xPDFsuite[15] for the XFEL data and the synchrotron data of $HfO_2$. This figure has been included to allow for a better assessment of the data normalization. Looking at F(Q) for the XFEL data, there seems to be a slowly oscillating background feature which could be the cause of the noisy features observed in the PDF at low r-values. This could indicate that there are uncorrected features possibly related to fluorescence if the fluorescence correction has been obscured by the mask employed (discussed in more detail in SI sec. 7 and 9). Fluorescence is much less of a problem for the synchrotron data as these were collected at much higher energies (~100 keV).

Despite the challenging data reduction process and the limited Q-range, the PDF obtained from the XFEL data of $HfO_2$ was modelled to obtain unit cell dimensions and crystallite sizes. Prior to modelling the PDF, the intensity dampening function ($Q_{damp}$) and the r-dependent peak shape correction ($Q_{broad}$) from the instrument had to be determined. Again, these instrumental contributions should ideally be determined by modelling a reference material in the same liquid jet setup, but here, the capillary $LaB_6$ sample had to be used, resulting in a $Q_{damp}$ of 0.0116(2) $Å^{-1}$ and $Q_{broad} = 0$ $Å^{-1}$ (refinement details in SI sec. 6). Using these parameters, the XFEL PDF could be modelled in TOPAS v. 7 (Figure 6),[13] refining the scale factor, zero parameter, and unit cell dimensions. The data quality was inadequate to refine atomic positions, so they were kept constant at literature values.[12] Similarly, the thermal parameters, B, were fixed at isotropic literature values of 0.45 $Å^2$ for all atoms. These B values seemed reasonable, judging from the peak shapes of the model (see inset in Figure 6). Note that the

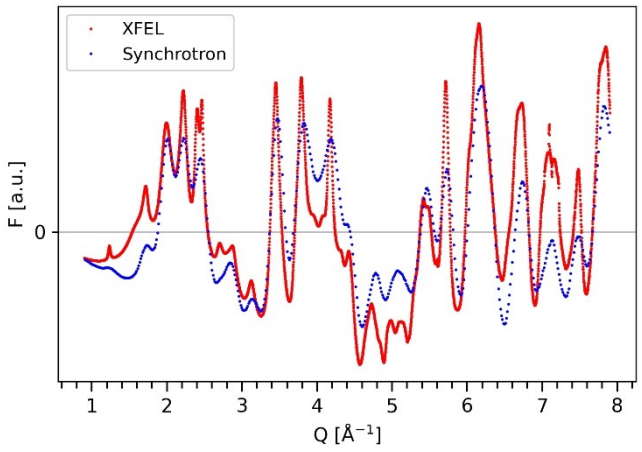


**Figure 5.** Reduced structure functions, F(Q), for the XFEL (red) and synchrotron (blue) data of $HfO_2$. A slowly oscillating background feature is observed in the XFEL PDF, which might be the cause of the noisy low r-range in the PDF.


© 2023 The Authors. ChemPhysChem published by Wiley-VCH GmbH

14397641, 2023, 23, Downloaded from https://chemistry-europe.onlinelibrary.wiley.com/doi/10.1002/cphc.202300407 by Cochrane Germany, Wiley Online Library on [15/12/2023]. See the Terms and Conditions (https://onlinelibrary.wiley.com/terms-and-conditions) on Wiley Online Library for rules of use; OA articles are governed by the applicable Creative Commons License

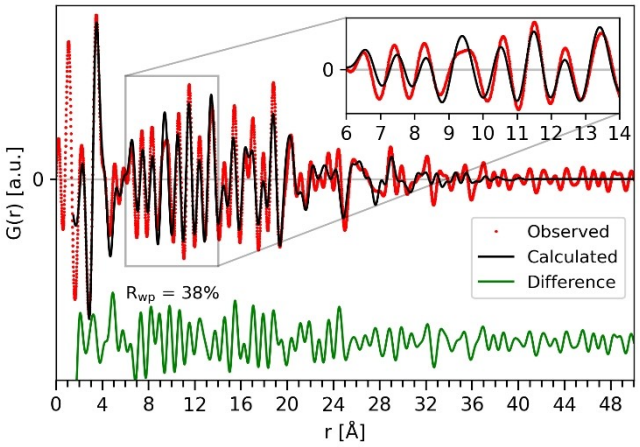


**Figure 6.** Measured (red) and modelled (black) XFEL PDF of $HfO_2$ and the difference curve (green). Notice that the region below the shortest distance of ~2 Å is mostly noise and thus not included in the model.

inability to refine atomic positions and thermal parameters is a common issue in PDF analysis. A spherical dampening parameter was refined to extract isotropic crystallite sizes, and the PDF was fitted in the r-range 1.5-60 Å, giving a final $R_{wp}$ of ~38%.

Many of the features in the PDF are clearly described by the model, but unsurprisingly, the fit is not perfect (Figure 6). The refined unit cell parameters were a = 5.161(1) Å, b = 5.204(2) Å, c = 5.342(2) Å, and β = 99.88(3)°, varying only slightly from the values obtained from the laboratory PXRD (see Table 1). The model in Figure 6 flattens out at around 37 Å, in agreement with the relatively small sizes expected for the nanoparticles, and the extracted crystallite size was ~4.4 nm, in good agreement with the laboratory data (Table 1). The quality of the fit is, of course, a result of the assumptions made during the data reduction process and the choice of parameters taking instrumental effects into account.

In summary, a PDF of a suspension of $HfO_2$ nanoparticles was obtained from femtosecond X-ray pulses using a liquid jet setup at the SACLA XFEL. Although the experimental setup was not optimized for PDF measurements, and the calibration as well as the background correction processes were challenging, many of the expected features were observed in the femtosecond PDF when comparing it to a reference synchrotron PDF. Modelling the XFEL PDF resulted in unit cell dimensions and particle sizes in agreement with literature as well as complimentary laboratory PXRD refinements on the same $HfO_2$ nanoparticles.

Although the accessible information was limited by a $Q_{max}$ of ~8 $Å^{-1}$, the result strongly indicates that high-quality PDFs of nanoparticle suspensions are within reach from XFEL sources if the experimental conditions are further optimized. Carefully designing improved calibration and background experiments will benefit the PDF, and the Q-range can be straightforwardly increased by using a higher X-ray energy and more optimal detector settings (tilting and vertical off-set). Optimizing the current detector setup at SACLA would in theory lead to a $Q_{max}$ ~14 $Å^{-1}$. Total X-ray scattering data with a $Q_{max}$ of 14 $Å^{-1}$ is shown to be sufficient to resolve the main features in the XFEL PDF of $HfO_2$, and such a $Q_{max}$ is not much lower than the data resolution obtained in many *in situ* studies of nanocrystal nucleation ($Q_{max}$ ~18 $Å^{-1}$).[4c,16]

In future experiments, a synchronized femtosecond laser may be used in a pump-probe fashion. This would allow photoexcitation or laser-induced heating to initiate ultrafast processes such as nanocrystal nucleation, phase transitions, or electronic excitations, and unlike pump-probe serial crystallography measurements,[17] femtosecond *in situ* PDF studies do not require crystalline samples. The present results provide substantial optimism for the future of femtosecond PDF studies. Indeed, a new direction in ultrafast structural dynamics will be enabled if "molecular movies" on the atomic scale can be obtained from amorphous, disordered, and crystalline samples using PDF analysis.

## Experimental Methods

The XFEL data of a suspension of $HfO_2$ nanoparticles were collected at SACLA. A 15.001 keV XFEL beam (λ = 0.8259 Å) with a less than 10 fs pulse duration was used. An 8-module MPCCD Octal Phase-III detector[11] was vertically offset by 42 mm at a Sample-to-Detector Distance (SDD) of ~42 mm. Aside from the inherent Self-Amplified Spontaneous Emission (SASE) process, no monochromatization was applied. The X-ray beam had an almost gaussian energy spread of 50 eV (FWHM). The exposure time was 1.0 ms, synchronized to the XFEL machine operated at 30 Hz. The sample was extruded through a 200 μm nozzle with a flow rate of 5.0 mL/min. The beam size was focused to ~2 μm×2 μm by *Kirkpatrick-Baez* focusing mirrors, and different Al or Si attenuators were used. For a more detailed description, see SI sec. 1.

$HfO_2$ nanoparticles were synthesized prior to the XFEL beamtime in a solvothermal synthesis.[4c] A precursor solution of $HfCl_4$ powder dissolved in methanol was heated to 175 °C in a Teflon-lined autoclave for 24 hours, and the resulting nanoparticles were washed with ethanol, dried, and ground in a mortar. PXRD data were measured using an in-house X-ray powder diffractometer (Rigaku Smartlab) having a Co source with a ~1 : 1 ratio of $\lambda_{K\alpha1}$ and $\lambda_{K\alpha2}$ radiation (1.78919 Å and 1.79310 Å, respectively). Data were measured in the 2θ-range 15–90° for ~26 min. For a more detailed description, see SI sec. 3.

## Supporting Information

The authors have cited additional references within the Supporting Information.[18,19]

## *Acknowledgements*

This work was supported by the Danish Center for Synchrotron and Neutron Research (DanScatt), the Villum Foundation, and JSPS KAKENHI (Grants No. JP17H05328, JP18H04499, JP19KK0132, JP20H04656 and JP21H05235). We gratefully acknowledge SPring-8 Angstrom Compact free electron LAser (SACLA) as well as Deutsches Elektronen-Synchrotron, DESY, a member of the Helmholtz Association (HGF), for providing the


© 2023 The Authors. ChemPhysChem published by Wiley-VCH GmbH

14397641, 2023, 23, Downloaded from https://chemistry-europe.onlinelibrary.wiley.com/doi/10.1002/cphc.202300407 by Cochrane Germany, Wiley Online Library on [15/12/2023]. See the Terms and Conditions (https://onlinelibrary.wiley.com/terms-and-conditions) on Wiley Online Library for rules of use; OA articles are governed by the applicable Creative Commons License

necessary experimental facilities. The experiments at BL2, SACLA were performed with the approval of the Japan Synchrotron Radiation Research Institute (JASRI), proposal number 2022A8003. We thank the beamline staff at SACLA for their help during our beamtime. Martin von Zimmermann and Ann-Christin Dippel are thanked for their assistance during beamtime at P21.1, PETRA III (DESY, Hamburg, Germany). Beamtime at DESY was allocated for proposal 20010116.

## Conflict of Interests

The authors declare no conflict of interest.

## Data Availability Statement

The data that support the findings of this study are available from the corresponding author upon reasonable request.

**Keywords:** femtosecond studies · nanoparticle nucleation · pair distribution function · structural dynamics · X-ray free electron laser

[1] E. A. Goodilin, P. S. Weiss, Y. Gogotsi, *ACS Nano* **2019**, *13*, 10879–10886.
[2] T. Egami, S. J. L. Billinge, *Underneath the Bragg peaks: structural analysis of complex materials*, Elsevier, **2012**, 2nd ed.
[3] a) B. S. Clausen, G. Steffensen, B. Fabius, J. Villadsen, R. Feidenhans'l, H. Topsøe, *J. Catal.* **1991**, *132*, 524–535; b) H. Jensen, M. Bremholm, R. P. Nielsen, K. D. Joensen, J. S. Pedersen, H. Birkedal, Y.-S. Chen, J. Almer, E. G. Søgaard, S. B. Iversen, B. B. Iversen, *Angew. Chem. Int. Ed.* **2007**, *46*, 1113–1116; c) K. M. Ø. Jensen, C. Tyrsted, M. Bremholm, B. B. Iversen, *ChemSusChem* **2014**, *7*, 1594–1611; d) P. Norby, *J. Am. Chem. Soc.* **1997**, *119*, 5215–5221; e) N. Pienack, W. Bensch, *Angew. Chem. Int. Ed.* **2011**, *50*, 2014–2034.
[4] a) C. Tyrsted, K. M. Ørnsbjerg Jensen, E. D. Bøjesen, N. Lock, M. Christensen, S. J. L. Billinge, B. Brummerstedt Iversen, *Angew. Chem. Int. Ed.* **2012**, *51*, 9030–9033; b) K. M. Ø. Jensen, M. Christensen, P. Juhas, C. Tyrsted, E. D. Bøjesen, N. Lock, S. J. L. Billinge, B. B. Iversen, *J. Am. Chem. Soc.* **2012**, *134*, 6785–6792; c) R. S. Christensen, M. Kløve, M. Roelsgaard, S. Sommer, B. B. Iversen, *Nanoscale* **2021**, *13*, 12711–12719; d) S. Birgisson, D. Saha, B. B. Iversen, *Cryst. Growth Des.* **2018**, *18*, 827–838.
[5] M. Roelsgaard, M. Kløve, R. Christensen, A. D. Bertelsen, N. L. N. Broge, I. Kantor, D. R. Sørensen, A.-C. Dippel, S. Banerjee, M. von Zimmermann, P. Glaevecke, O. Gutowski, M. R. V. Jørgensen, B. B. Iversen, *J. Appl. Crystallogr.* **2023**, *56*, 1–8.
[6] a) E. J. Mascarenhas, M. Fondell, R. Büchner, S. Eckert, V. Vaz da Cruz, A. Föhlisch, *Phys. Chem. Chem. Phys.* **2022**, *24*, 17979–17985; b) J. Agarwal, C. J. Stanton Iii, T. W. Shaw, J. E. Vandezande, G. F. Majetich, A. B. Bocarsly, H. F. Schaefer Iii, *Dalton Trans.* **2015**, *44*, 2122–2131.
[7] P. Willmott, *An Introduction to Synchrotron Radiation: Techniques and Applications*, John Wiley & Sons Ltd, **2019**, 2nd ed.
[8] J. Als-Nielsen, D. McMorrow, *Elements of Modern X-ray Physics*, John Wiley & Sons, **2011**, 2nd ed.
[9] a) H. N. Chapman, P. Fromme, A. Barty, T. A. White, R. A. Kirian, A. Aquila, M. S. Hunter, J. Schulz, D. P. DePonte, U. Weierstall, R. B. Doak, F. R. N. C. Maia, A. V. Martin, I. Schlichting, L. Lomb, N. Coppola, R. L. Shoeman, S. W. Epp, R. Hartmann, D. Rolles, A. Rudenko, L. Foucar, N. Kimmel, G. Weidenspointner, P. Holl, M. Liang, M. Barthelmess, C. Caleman, S. Boutet, M. J. Bogan, J. Krzywinski, C. Bostedt, S. Bajt, L. Gumprecht, B. Rudek, B. Erk, C. Schmidt, A. Hömke, C. Reich, D. Pietschner, L. Strüder, G. Hauser, H. Gorke, J. Ullrich, S. Herrmann, G. Schaller, F. Schopper, H. Soltau, K.-U. Kühnel, M. Messerschmidt, J. D. Bozek, S. P. Hau-Riege, M. Frank, C. Y. Hampton, R. G. Sierra, D. Starodub, G. J. Williams, J. Hajdu, N. Timneanu, M. M. Seibert, J. Andreasson, A. Rocker, O. Jönsson, M. Svenda, S. Stern, K. Nass, R. Andritschke, C.-D. Schröter, F. Krasniqi, M. Bott, K. E. Schmidt, X. Wang, I. Grotjohann, J. M. Holton, T. R. M. Barends, R. Neutze, S. Marchesini, R. Fromme, S. Schorb, D. Rupp, M. Adolph, T. Gorkhover, I. Andersson, H. Hirsemann, G. Potdevin, H. Graafsma, B. Nilsson, J. C. H. Spence, *Nature* **2011**, *470*, 73–77; b) J.-P. Colletier, G. Schirò, M. Weik, *X-Ray Free Electron Lasers: A Revolution in Structural Biology*, Springer International Publishing, **2018**.
[10] T. Ishikawa, H. Aoyagi, T. Asaka, Y. Asano, N. Azumi, T. Bizen, H. Ego, K. Fukami, T. Fukui, Y. Furukawa, S. Goto, H. Hanaki, T. Hara, T. Hasegawa, T. Hatsui, A. Higashiya, T. Hirono, N. Hosoda, M. Ishii, T. Inagaki, Y. Inubushi, T. Itoga, Y. Joti, M. Kago, T. Kameshima, H. Kimura, Y. Kirihara, A. Kiyomichi, T. Kobayashi, C. Kondo, T. Kudo, H. Maesaka, X. M. Maréchal, T. Masuda, S. Matsubara, T. Matsumoto, T. Matsushita, S. Matsui, M. Nagasono, N. Nariyama, H. Ohashi, T. Ohata, T. Ohshima, S. Ono, Y. Otake, C. Saji, T. Sakurai, T. Sato, K. Sawada, T. Seike, K. Shirasawa, T. Sugimoto, S. Suzuki, S. Takahashi, H. Takebe, K. Takeshita, K. Tamasaku, H. Tanaka, R. Tanaka, T. Tanaka, T. Togashi, K. Togawa, A. Tokuhisa, H. Tomizawa, K. Tono, S. Wu, M. Yabashi, M. Yamaga, A. Yamashita, K. Yanagida, C. Zhang, T. Shintake, H. Kitamura, N. Kumagai, *Nat. Photonics* **2012**, *6*, 540–544.
[11] T. Kameshima, S. Ono, T. Kudo, K. Ozaki, Y. Kirihara, K. Kobayashi, Y. Inubushi, M. Yabashi, T. Horigome, A. Holland, K. Holland, D. Burt, H. Murao, T. Hatsui, *Rev. Sci. Instrum.* **2014**, *85*.
[12] R. Ruh, P. W. R. Corfield, *J. Am. Ceram. Soc.* **1970**, *53*, 126–129.
[13] A. Coelho, *J. Appl. Crystallogr.* **2018**, *51*, 210–218.
[14] https://11bm.xray.aps.anl.gov/absorb/absorb.php (25/8-2023).
[15] X. Yang, P. Juhas, C. L. Farrow, S. J. Billinge, *arXiv preprint arXiv:1402.3163* **2014**.
[16] E. D. Bøjesen, B. B. Iversen, *CrystEngComm* **2016**, *18*, 8332–8353.
[17] L. J. Støckler, L. Krause, B. Svane, K. Tolborg, B. Richter, S. Takahashi, T. Fujita, H. Kasai, M. Sugahara, I. Inoue, E. Nishibori, B. B. Iversen, *IUCrJ* **2023**, *10*, 103–117.
[18] C. Prescher, V. B. Prakapenka, *High Pressure Res.* **2015**, *35*, 223.
[19] G. Ning, R. L. Flemming, *J. Appl. Crystallogr.* **2005**, *38*, 757.

Manuscript received: June 20, 2023
Revised manuscript received: September 10, 2023
Accepted manuscript online: September 13, 2023
Version of record online: October 6, 2023


© 2023 The Authors. ChemPhysChem published by Wiley-VCH GmbH

14397641, 2023, 23, Downloaded from https://chemistry-europe.onlinelibrary.wiley.com/doi/10.1002/cphc.202300407 by Cochrane Germany, Wiley Online Library on [15/12/2023]. See the Terms and Conditions (https://onlinelibrary.wiley.com/terms-and-conditions) on Wiley Online Library for rules of use; OA articles are governed by the applicable Creative Commons License